

## ✿ Interpreting the Appearance of Dispersed Systems:

### I. Model Dispersions of Polymer Latex Microspheres

E.I. FRANSES<sup>1</sup>, L.E. SCRIVEN, W.G. MILLER and H.T. DAVIS, Departments of Chemical Engineering and Materials Science and of Chemistry, University of Minnesota, Minneapolis, MN 55455

#### ABSTRACT

Measurements of total absorbance at wavelengths 350-780 nm of aqueous dispersions of polymer latex microspheres of diameters 0.091  $\mu\text{m}$ , 0.254  $\mu\text{m}$ , 0.325  $\mu\text{m}$ , and 1.10  $\mu\text{m}$  were used to interpret systematic observations of them. Light scattering dissymmetries and scattering ratios of dispersions of the 0.091  $\mu\text{m}$  microspheres were measured at varying concentration and path length at 546 nm and 436 nm. Spectroturbidimetry and observations were also made in binary mixtures of the above particle sizes and in dispersions of microspheres with added dye, the sodium salt of methyl red. For absorbance due to scattering,  $A_{\text{scat}}$ , exceeding 0.04 but not 2, the absorbance and its wavelength dependence yield reliable estimates of particle size, even though the dissymmetry and the scattering ratio do not. Observations of nonabsorbing systems under ordinary illumination are most reliably interpreted with  $0.1 < A_{\text{scat}} < 1$ , i.e., when the systems look translucent to translucent-turbid, even though multiple scattering predominates in this range. That the Tyndall effect, or a variant of it when absorption is important, is visible implies that particles smaller than 0.1  $\mu\text{m}$  are present. To estimate particle sizes in milky dispersions in which  $A > 2$ , it is necessary to decrease the path length — or the concentration, if tolerable — so that the absorbance falls in that optimal range. Outside this range, the literature rules are unreliable. Because observers and illumination conditions vary among laboratories, it seems essential that model systems such as the microspheres and the dye employed here be used to simulate scattering and absorption features of dispersed systems. By direct comparisons of model systems to systems of interest, observations can be standardized and interpretation of appearances can become less subjective. Moreover, combining observations with spectroturbidimetry provides a much more potent tool for estimating sizes simply and quickly.

#### INTRODUCTION

The visual appearance of macroscopically homogeneous liquids is often used as a criterion for initially classifying them as solutions, micellar solutions, microemulsions, macroemulsions, dispersions, etc. (1,2). Simple observations can be useful in studying phase behavior, interfacial tension, and nonequilibrium of dispersed and colloidal systems. Observations can quickly provide qualitative information that is valuable in any screening program. And, most important, they can indicate directions for more detailed scientific investigations.

Various published rules for estimating particle size in nonabsorbing emulsions and microemulsions are shown in Table I. In the phenomenon called the Tyndall effect, if a nonabsorbing system is illuminated by white light, it appears blue by scattering light and orange-red by transmitted light

(3). This effect has been used extensively to detect Rayleigh scatterers. These are particles with dimensions much smaller than the wavelength of the light used; they are generally smaller than 0.1  $\mu\text{m}$  (3). There seems to be no detailed account of how the reported rules depend on path length of sample, concentration of scatterers, extent of multiple scattering, amount of chromophore absorption, and intensity of light source.

To evaluate these rules and devise improved ones, we made spectroturbidimetry experiments and visual observations on a series of aqueous dispersions of polymer latex microspheres. Such dispersions are excellent model systems for testing quantitatively theories, equipment, and procedures concerning colloidal particles (4). Latex microspheres of highly uniform size are commercially available in diameters ranging from 0.09 to many micrometers. The particles can remain in stable suspension for weeks and months, although they eventually agglomerate.

In Part I we review briefly the important principles of light scattering, spectroturbidimetry, and spectrophotometry, which form the basis for interpreting visual appearances. We investigate by spectroturbidimetry the three most important scattering regimes, Rayleigh, Rayleigh-Debye-Gans, and Mie, by using appropriate monodisperse particle sizes. We also examine certain single- and multiple-scattering dispersions by light scattering. We use mixtures of monodisperse sizes to simulate size distributions, which are

TABLE I

Literature Rules for Interpreting Appearance of Dispersions

(a) Prince (1)		
Appearance	Tyndall effect	Average particle size ( $\text{\AA}$ )
"Dead white"	None	> 5000
"White-gray"	Weak	1000-3000
"Gray-translucent"	Strong	100-1400
"Clear transparent"	None	<100
(b) Griffin (2)		
Appearance	Average particle size ( $\text{\AA}$ )	
"Distinguishable phases"	Macroglobules	
"Milky white"	> 10000	
"Blue-white"	1000-10000	
"Gray-semitransparent"	500-1000	
"Transparent"	<500	

<sup>1</sup>Current address: School of Chemical Engineering, Purdue University, West Lafayette, IN 47907.

present in most practical systems. Moreover, we test dispersions with added dye to see how the interpretation of spectroturbidimetry and visual appearance must be modified when there is chromophore absorption in addition to scattering. Absorbance measurements enable us to evaluate the visual observations and analyze their pitfalls. We conclude that the previously published rules are not always reliable. We suggest new rules and discuss their limitations. The limitations are fewer if observations are combined with spectroturbidimetry.

In Part II we outline simple rules, in guide form, for quick and careful visual observations of surfactant systems (5). We show that the dispersions of polymer latex microspheres are indeed good models of surfactant dispersions. And finally we illustrate the usefulness of the guide by reporting observations of various surfactant systems we examined in the course of studies of phase behavior, interfacial tension, and dispersion stability (6-8).

## THEORY

### Absorption and Scattering

For a parallel light beam of incident intensity  $I_0$  and transmitted intensity  $I$ , the transmittance  $T$  is defined as  $I/I_0$  and the absorbance  $A$  as  $-\log_{10} T$ . Usually  $T < 1$ , and hence  $A > 0$ . The attenuation of incident light is due to chromophore absorption ( $A_{\text{abs}}$ ), or scattering ( $A_{\text{scat}}$ ), or both. The specific absorbance due to chromophore absorption is  $\epsilon \equiv A_{\text{abs}}/l c$ , where  $c$  is the molar concentration (mol/L) and  $l$  is the path length (cm). According to the Beer-Lambert law,  $\epsilon$  is independent of the concentration and the state of aggregation of the chromophores. Relatively minor deviations can arise from effects of complex formation or variation of solvent polarity (9,10). By contrast,  $A_{\text{scat}}$ , which measures the total scattering in all directions, depends strongly on particle size and may vary with concentration. In systems in which the chromophores occupy a small volume fraction of the scattering particle or aggregate, the scattering and absorption efficiencies of the particle should not affect each other. Therefore, the absorbances due to scattering and absorption should be additive  $A/l c = A_{\text{abs}}/l c + A_{\text{scat}}/l c$ . Hence, by measuring the total absorbance  $A$  and  $A_{\text{abs}}$  the total scattering can be determined by difference.

### Single Scattering

In single scattering, less than ca. 10% of the incident intensity is scattered (see next subsection). Thus the sample is exposed to virtually the same incident intensity over the whole path length, provided of course that chromophore absorption is also small. For light wavelength  $\lambda_0$  (in vacuo) the scattering intensity  $i(\theta)$  at a scattering angle  $\theta$  depends on  $\lambda_0, \theta$ , and the ratio  $m$  of the refractive index  $n_p$  of the particle or aggregate relative to the refractive index  $n_0$  of the surrounding solvent:  $m \equiv n_p/n_0$ . For spherical particles of diameter  $d$ , their dimensionless size is

$$\alpha \equiv \pi d/\lambda \quad [1]$$

where  $\lambda = \lambda_0/n_0$ .

The scattering intensity and its state of polarization are complex functions of  $\alpha, \lambda_0, \nu, m$ , and the state of polarization of the incident light (3). Simple limiting cases that are important for colloidal sizes ( $< 0.2 \mu\text{m}$ ) are presented

below. One can use polarized (e.g., vertically,  $I_0^V$ , or horizontally,  $I_0^H$ ) or unpolarized ( $I_0^U$ ) incident light and measure either the total scattered intensities ( $i_V, i_H$  and  $i_U$  or  $i_\theta$ , respectively) or vertical or horizontal components of the scattered light.

In the Rayleigh scattering regime, the external field induces a dipole that oscillates in phase with the external field, which is virtually homogenous over the extent of the scattering particle. Rayleigh scattering occurs when the particle size is much smaller than the wavelength and when the static polarization is established in a time short compared to the period, i.e., when (Ref. 11, p. 75)

$$\alpha \ll 1 \text{ and } \alpha |m| \ll 1 \quad [2]$$

Provided  $|m| < 2$  and  $d < \lambda/10$ , these conditions are satisfied adequately in practice. For particles in this regime,

$$i_V/I_0^V = 2 K M c/r^2 \quad [3]$$

$$i_H/I_0^H = 2 K M c \cos^2 \theta / r^2 \quad [4]$$

and

$$i_U/I_0^U = K M c (1 + \cos^2 \theta) / r^2 \quad [5]$$

where  $K$  is an optical constant,  $K \equiv 2\pi^2 n_0^2 (dn/dc)^2 / (N_A \lambda^4)$ , and  $M$  is the molecular weight of the particles,  $N_A$  is Avogadro's number, and  $dn/dc$  is the specific refractive index increment,  $dn/dc \equiv \lim (n - n_0)/c$  as  $c \rightarrow 0$  (12).

Equations 3-5 apply to suspensions so dilute that the particles scatter independently of each other. As concentration rises, dependent scattering, or interparticle interference, becomes important. The following equation can describe the concentration dependence (12):

$$Kc/R_\theta = 1/M + 2Bc + 3Cc^2 + \dots \quad [6]$$

where  $R_\theta$ , the Rayleigh ratio, is defined as

$$R_\theta \equiv r^2 i_U / [I_0^U (1 + \cos^2 \theta)] = r^2 i_V / (2I_0^V) = r^2 i_H / (2I_0^H) \quad [7]$$

and  $B$  and  $C$  are the second and third virial coefficients (12).

If  $i_T$  is the fraction of the incident intensity that is scattered, i.e.,

$$i_T \equiv (I_0 - I)/I_0 = 1 - T = l(1/I_0) \int_0^\pi 2\pi r^2 i_\theta \sin \theta d\theta \quad [8]$$

and  $\tau$  is the turbidity  $\tau \equiv -\ln_e (I/I_0) = -\ln T$ , then  $\tau = \ln(1 - i_T)$  and  $\tau = 2.303 A_{\text{scat}}$ . For single scattering, as explained above,  $i_T \ll 1$ . It follows that  $\tau \approx i_T$  and

$$R_\theta = (3/16\pi) \tau / l \quad [9]$$

Thus measuring  $A_{\text{scat}}/l$  for single scattering, the Rayleigh ratio can be determined.

Single scattering from optically isotropic Rayleigh spheres is completely polarized for polarized incident light. The direction of polarization can differ from that of the incident light. With polarized incident light, single scattering from anisotropic or nonspherical Rayleigh particles can, however, be partially unpolarized (13). A useful measure of size, shape, orientation, and extent of multiple scattering is the scattering ratio, which is defined as

$$\rho_U(\theta) \equiv i_H(\theta)/i_V(\theta) \quad [10]$$

For isotropic Rayleigh spheres  $\rho_U(90^\circ) = 0$ , according to equations 3 and 4. For nonspherical Rayleigh particles  $\rho_U(90^\circ) > 0$ . For isotropic or spherical particles that are not in the Rayleigh regime  $\rho_U(90^\circ) > 0$  in most cases, because

the oscillating dipoles are not parallel to the electric vector of the incident light.

In the Rayleigh-Debye-Gans regime, each volume element gives Rayleigh scattering and does so independently of the other volume elements (Ref. 11, p. 85). The refractive index differs little from that of the surrounding medium and phase shift  $\alpha|m-1|$  is small, i.e.,

$$|m-1| \ll 1 \text{ and } \alpha|m-1| \ll 1 \quad [11]$$

Hence  $\alpha$  can be larger than 1 if  $|m-1|$  is sufficiently smaller than 1. Because of destructive intraparticle interference, the Rayleigh ratio, which is independent of angle in Rayleigh scattering, can vary with scattering angle  $\nu$ ; when  $d < \lambda/2$ , it decreases monotonically over the whole range of angles 0-180° (14). A convenient measure of the angular dependence is the dissymmetry

$$Z(\theta) \equiv i(\theta)/i(180^\circ - \theta) \quad [12]$$

In this regime,  $Z(\theta) > 1$ . Dissymmetry measurements and tabulated calculations (14) can provide the particle size if the particle shape or configuration is known from other evidence.

If neither the conditions (2) nor (11) are satisfied, the scattering is called Mie scattering after Mie's theory, which applies to spheres at any value of  $m$  and  $\alpha$ . In this regime, the scattering intensity is concentrated mainly at small forward angles and can have maxima and minima as angle increases. The turbidity can increase or decrease and have maxima and minima as size increases or as wavelength decreases (15,16).

The wavelength dependence of scattering by dispersion of particles can be represented by the exponent  $g$  defined from  $\tau \propto \lambda_0^{-g}$ , i.e.,

$$g \equiv -d \log \tau / d \log \lambda_0 \quad [13]$$

The value of  $g$  is a sensitive indicator of the value of the dimensionless size  $\alpha$  if the refractive index ratio  $m$  is known. It is also important for relating spectroturbidimetry to appearance because it determines the scattering colors. In the Rayleigh regime, the dependence of the turbidity on the wavelength is the strongest (3).

$$\tau = \frac{24\pi^3 c}{N_A} \frac{m^2 - 1}{m^2 + 2} \frac{Mn_0^4}{\rho_p^2 \lambda_0^4} \quad [14]$$

Because  $n_0$  and  $m$  vary a little with wavelength,  $g$  can be slightly larger than 4. In the Rayleigh-Debye-Gans regime, the exponent  $g$  is less than 4 and decreases with decreasing wavelength. In the Mie scattering regime,  $g$  is smaller than 4 and can be negative. The smaller the value of  $|m-1|$ , the larger the range of  $\alpha$  in which the turbidity increases with increasing size, i.e.,  $g$  is positive (15,16). It is useful to estimate  $g$  and determine roughly the scattering regime by plotting  $A\lambda_0^4$  and  $A\lambda_0^2$  versus  $\lambda_0$ . For Rayleigh scattering, the product  $A_{\text{scat}}\lambda_0^4$  is constant or increases slowly. A value of  $g$  less than 4 indicates that some or all particles in the dispersion are not Rayleigh scatterers. According to published calculations, if  $g$  ranges from 2 to 4 and  $m < 1.3$ , then  $\alpha$  is less than 2.5 (15). Mie scattering is implied when  $g < 2$ . By analogy to the dissymmetry, which measures the departure of scattering from the Rayleigh limit, the particle dissipation factor is defined as

$$Q \equiv \tau/\tau_0 \quad [15]$$

where  $\tau$  and  $\tau_0$  are the turbidities in the presence and absence, respectively, of intraparticle interference. Chromophore absorption can depend much more strongly than scattering on wavelength. Whereas the product  $A_{\text{scat}}\lambda_0^4$  can increase only slightly with decreasing wavelength,  $A_{\text{abs}}\lambda_0^4$  can increase substantially (recall that the total absorbance  $A = A_{\text{scat}} + A_{\text{abs}}$ ). Hence, when  $A\lambda_0^4$  increases strongly with decreasing wavelength,  $A_{\text{abs}}$  must be significant.

Spectroturbidimetry, plots of  $A$  or  $A\lambda_0^4$  or  $A\lambda_0^2$  versus  $\lambda_0$ , is not as sensitive an indication of sizes as are measurements of the scattering intensity versus angle. In the visible wavelength range, 800-350 nm, the scattering parameter  $\alpha (\equiv \pi d/\lambda)$  varies less than does the angular scattering parameter  $(\pi d/\lambda) \sin(\theta/2)$  in the angular range 30-150°, which is commonly scanned. Spectroturbidimetry, however, is affected much less by multiple scattering, i.e., when  $A > 0.04$ , as explained in the next section. Hence, when  $A < 0.04$ , measurements of the angular dependence are undoubtedly superior; when  $A > 0.04$ , spectroturbidimetry is preferable.

### Multiple Scattering

As the turbidity  $\tau$  increases, an increasing fraction of scattered light is scattered repeatedly before it reaches the detector. Dispersed particles are exposed to both the attenuated incident beam and to the scattered light. If the specific turbidity  $\tau/c$  is independent of concentration, multiple scattering is almost certainly insignificant (11). However,  $\tau/c$  can depend on concentration because of interparticle interactions (12), even when single scattering prevails. If  $\tau/l$  is independent of the path length  $l$  at a fixed concentration, then multiple scattering is unimportant. Thus the length-dependence criterion is more reliable than the concentration-dependence criterion. Van de Hulst suggests using the turbidity as the criterion: if  $\tau < 0.1$  ( $A \lesssim 0.04$ ), single scattering prevails; if  $0.04 \lesssim A_{\text{scat}} < 0.13$ , a correction for multiple scattering is needed; and if  $A_{\text{scat}} > 0.13$ , multiple scattering dominates (11).

Multiple scattering redistributes in space the singly scattered light. The angular dependence of multiply scattered light becomes more uniform with increasing extent of multiple scattering (17). In the Rayleigh-Debye-Gans regime, the dissymmetry (Equation 12) increases. Moreover, the degree of depolarization increases as multiple scattering gains in importance (18). The scattering ratio  $\rho_u$  (90°) approaches 1, from below or from above, as in certain cases of Mie scattering. This means that the scattering light is mainly unpolarized.

The problem of deducing the particle size from the angular dependence of multiple scattering is difficult to intractable when particle sizes are distributed. Only if there is strong evidence that the particles are of uniform size and shape is it worth the computational effort to match calculations to multiple-scattering data in order to estimate particle size. On the other hand, multiple scattering will affect the turbidity per unit path length  $\tau/l$  and its wavelength dependence much less than it does the angular dependence. The reason is as follows. If the incident beam is very thin and parallel and if the distance between the sample and the detector is very large, little scattered or rescattered light reaches the detector. The turbidity is then strictly proportional to the path length. The incident beam, however, may

have some divergence and it certainly has a finite cross-section. The light scattered at small angles in the cone of acceptance that the detector subtends the sample enhances the measured transmitted intensity and thus introduces an error in the measured absorbance. The error is of course larger, the larger the angle of acceptance (19,20).

For small  $\alpha$ , corresponding to Rayleigh and Rayleigh-Debye-Gans scattering, the angular distribution of scattered light is quite uniform. The fraction of the total scattered light which reaches the detector is then about equal to  $f$ , the fraction (in steradians divided by  $4\pi$ ) of the solid angle subtended by the detector at the center of the sample. If only the angle-of-acceptance error is considered, the measured absorbance  $A^*$  is

$$A^* = -\log_{10} 10^{-A} (1-f) + f \quad [16]$$

where  $A$  is the true absorbance.

For the typical absorbance range 0-2 of a commercial spectrophotometer and a typical solid angle fraction  $f = 0.004$ , the relative error in  $A$  is less than 7.3%; when  $A < 1$  and  $f = 0.004$ , the error is less than 1.6%. Consequently, at  $A < 2$  and  $f < 0.004$  in Rayleigh and Rayleigh-Debye-Gans scattering the turbidity is affected by less than 7.3% at all wavelengths. The error in the wavelength exponent  $g$ , which is a "fingerprint" of the particle-size distribution, is small and often tolerable. The farther the detector is placed from the sample, the smaller the error and the larger the absorbance range that can be interpreted in terms of the single-scattering theory.

In Mie scattering, most of the scattered light is concentrated at small angles. The fraction of the total scattering which reaches the detector is much larger than  $f$ . The angle-of-acceptance error is larger for Mie scattering than for Rayleigh-Debye-Gans scattering and can be important even when  $A < 0.2$ . As  $A$  increases with decreasing wavelength, the asymmetry in the angular distribution of single scattering increases, as in some important cases of Mie scattering. The error in the absorbance may decrease, however, as the extent of multiple scattering increases. Thus the relative error in absorbance depends little on the wavelength, and the wavelength dependence yields a size distribution "fingerprint" which is almost identical to that when single scattering prevails.

## MATERIALS AND PROCEDURES

The microspheres used are characterized in Table II. The as-received, ~10 wt % latex, dispersions of sizes 0.091, 0.254, 0.325, and 1.10  $\mu\text{m}$  were diluted to stock dispersions of concentrations 500-1500 ppm, which were subsequently diluted further. The concentrations of the samples examined were known accurately on a relative but not on an absolute basis. The dependence of absorbance on size and concentration gave no indication that any significant aggregation of microspheres occurred before the measurements. All measured absorbances at 780-400 nm were due to scattering. All samples were diluted with an aqueous solution of 0.21 wt % sodium dodecylsulfate (SDS). The absorbance arising from the surfactant was less than  $0.001 \text{ cm}^{-1}$  at all wavelengths and hence was neglected. The surfactant improved substantially the stability of the dispersions of the 0.091  $\mu\text{m}$  microspheres; no visible particles were observed in such dispersions over more than a month. On standing,

the further diluted dispersions of 0.325  $\mu\text{m}$  and 1.10  $\mu\text{m}$  microspheres flocculated and settled faster than the stock dispersions. Moreover, after months, a crystalloidal precipitate was seen. This precipitate was visually and microscopically similar to the precipitate observed when only SDS was present. We believe that the precipitate arises from SDS hydrolysis. For these reasons, different concentrations of dispersions of the same particle size were tested the same day and all samples were tested within ten days after dilution.

Cary 14 and Cary 15 spectrophotometers were used. Their important features were identical. The solid angle fraction  $f$  subtended by the detector at the sample was less than 0.004. Specific absorbances  $A/l$  measured at 1 cm path length were used to calculate absorbances at other path lengths at which the effects of multiple scattering on absorbance were unimportant and hence  $A$  was proportional to  $l$ . A SOFICA light scattering photogoniometer 42000, Model 701, was used to measure dissymmetries and scattering ratios.

The water-soluble dye used was the sodium salt of methyl red (Eastman Kodak Co.). The aqueous solutions ranged in color from yellow to red, depending on concentration and path length.

For visual observations, cylindrical vials of internal diameter 2 cm were used. They were filled to 6-cm depth so that observations could be made at two different path lengths. Smaller vials of diameter 1 cm were also used; they were filled to 2 cm. Observations were made with normal laboratory illumination with a fluorescent light source. Many of the 2-cm vials were photographed against a black background using Kodak EPT 4 ASA 50 film and a matched Tungsten 3200 K lamp. An ultraviolet (UV) filter was used in the camera. Among photographs with different exposure times, the one with colors and translucency closest to the visual appearance under the same illumination source was chosen. The exposure time was normally 1/15 sec.

The light reaching the eye is a mixture of light scattered from the sample at different scattering angles and that transmitted through the sample; the proportions depend on the relative position of light source, sample, and observer. For this reason, in tables of observations below we use the entry color of scattered on transmitted light. Only if one uses high intensity illumination, a collimated incident beam, and a dark background, and observes a narrow range of scattering angles can one observe solely the scattered light.

## RESULTS AND DISCUSSION

### Dispersions of Microspheres of One Size

We measured the absorbance spectra of the following dispersions: 0.091  $\mu\text{m}$ : 21, 120, and 1300 ppm; 0.254  $\mu\text{m}$ : 18 and 48 ppm; 0.325  $\mu\text{m}$ : 70 and 900 ppm; and 1.10  $\mu\text{m}$ : 4.6, 18, and 65 ppm.

With each size of microspheres, the specific absorbance  $A/c$  was at all wavelengths independent of concentration within the experimental accuracy. Since the absolute uncertainty in absorbance was about the same in all measurements, the relative uncertainty was higher, the lower the absorbance. With the 0.091  $\mu\text{m}$  microspheres, the maximum variation of  $A/c$  with concentration was 5% for absorbances 0.02-2; with the 0.254  $\mu\text{m}$  microspheres, the specific absorbances at 48 ppm were ca. 10% lower than

## APPEARANCES OF MODEL DISPERSIONS

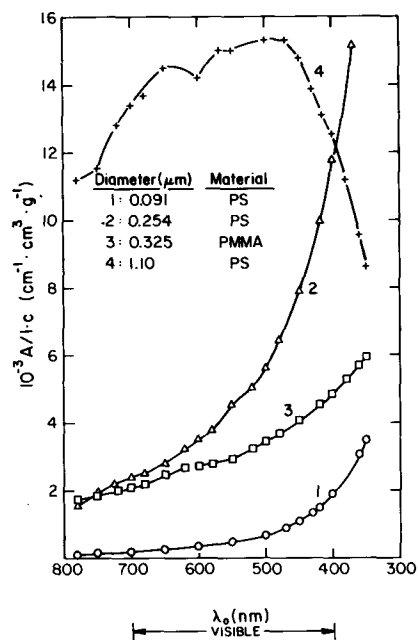


FIG. 1A. Absorbance of dispersions of polymer latex microspheres.

those at 18 ppm at all wavelengths. Since some crystalloidal particles which could contribute to the scattering were seen in the low-concentration sample, it is not certain that the discrepancy is significant. With the 0.325  $\mu\text{m}$  microspheres, the specific absorbances at 900 ppm were similarly 10-20% smaller than at 70 ppm. With the 1.10  $\mu\text{m}$  microspheres, the specific absorbance also decreased by 1 to 8% from 4.6 to 18 ppm and by an additional -2 to 7% from 18 to 65 ppm. We report spectra of the specific absorbances at only one concentration for each size - 1300 ppm for the 0.091  $\mu\text{m}$ , 48 ppm for the 0.254  $\mu\text{m}$ , 70 ppm for the 0.325  $\mu\text{m}$ , and 18 ppm for the 1.10  $\mu\text{m}$  microspheres - since the spectra at the other concentrations had the same shape.

Because the spectrum of specific absorbance was the same whether or not there was multiple scattering, we concluded that the effects of multiple scattering and angle of acceptance on absorbance were negligible in our apparatus, for absorbances up to 2 and for particle sizes up to 1.1  $\mu\text{m}$  at least. Hence in these ranges the absorbance is proportional to the path length, with deviations smaller than 20%. For particles having refractive index ratios relatively to water smaller than 1.2, that of the polystyrene spheres used, the scattering is less concentrated in forward angles. Thus we feel that sizes larger than 1.1  $\mu\text{m}$  can be reliably probed by

TABLE II

Features of Polymer Latex Microspheres Used

Sample	Nominal diameter <sup>a</sup> ( $\mu\text{m}$ )	Standard deviation ( $\mu\text{m}$ )	Latex material	$m^b$	$dn_0/\lambda_0$		$\alpha = \pi dn_0/\lambda_0$	
					$\lambda_0 = 780 \text{ nm}$	$\lambda_0 = 400 \text{ nm}$	$\lambda_0 = 780 \text{ nm}$	$\lambda_0 = 400 \text{ nm}$
1	0.091	0.0058	PS <sup>c</sup>	1.20	0.155	0.30	0.48	0.94
2	0.254	0.0025	PS <sup>d</sup>	1.20	0.43	0.85	1.35	1.67
3	0.325	unavailable	PMMA <sup>e</sup>	1.13	0.56	1.08	1.76	3.39
4	1.10	0.0059	PS <sup>c</sup>	1.20	1.88	3.67	5.91	11.53

<sup>a</sup>Values, provided by the manufacturer, were almost certainly determined by electron microscopy.

<sup>b</sup>Refractive index of polymer particle relative to water,  $m \equiv n_p/n_0$ ; it depends slightly on wavelength (21).

<sup>c</sup>Polystyrene, from Dow Diagnostics: 0.091  $\mu\text{m}$ , lot #2F5R; 1.10  $\mu\text{m}$  lot #2F8R.

<sup>d</sup>Polystyrene, carboxylate-modified surface, from Dow Diagnostics, lot #6H3K.

<sup>e</sup>Poly (methyl methacrylate), from Polysciences, Inc.

TABLE III

Effect of Increasing Absorbance, i.e., of Extent of Multiple Scattering, on Light Scattered from Polymer 0.091  $\mu\text{m}$  Microspheres

Concentration (ppm)	$A^a$	$\lambda_0 = 546 \text{ nm (green)}$			$\lambda_0 = 436 \text{ nm (blue)}$			
		$Z(45)^b$	$Z(30)^b$	$\rho_U^c$	$A^a$	$Z(45)^b$	$Z(30)^b$	$\rho_U^c$
2.06	0.0012	1.32	1.50	0.022	0.0029	1.40	1.60	0.022
3.2	0.0018				0.0044		1.57	
4.9	0.0021	1.26	1.43	0.025	0.0069	1.39	1.56	0.024
5.5	0.0031				0.0077		1.58	
10.8	0.0061				0.0152		1.52	
13.8	0.0080	1.27	1.37	0.022	0.0195	1.39	1.48	0.027
20.5	0.0120				0.0288		1.52	
51.0	0.029	1.25	1.35	0.035	0.072	1.37	1.50	1.05
315	0.12	1.22	1.29	0.09	0.295	1.17	1.20	0.18
315	0.18	1.11	1.21	0.11	0.445	1.16	1.25	0.24

<sup>a</sup>Total absorbance due to scattering: calculated from the specific absorbance  $A/lc$ , measured by a spectrophotometer, and the radius of the scattering cell (1.2 cm in most cases).

<sup>b</sup>Dissymmetry  $Z(\theta) \equiv i(\theta)/i(180 - \theta)$ ;  $i$  is scattered intensity and  $\theta$  is scattering angle.

<sup>c</sup>Scattering ratio  $\rho_U(90^\circ) \equiv i_H(90^\circ)/i_V(90^\circ)$ ;  $i_H$  and  $i_V$  are total scattered intensities for horizontally and vertically polarized incident light.

TABLE IV

Effect of Multiple Scattering on Apparent Particle Diameter Calculated from Dissymmetries

$\lambda_0$ (nm)	Z(45) <sup>a</sup>	D/ $\lambda$ <sup>b</sup>	D( $\mu\text{m}$ ) <sup>c</sup>
546	1.32	0.22	0.088
546	1.22	0.19	0.078
546	1.11	0.14	0.057
436	1.40	0.24	0.078
436	1.37	0.23	0.076
436	1.16	0.16	0.052

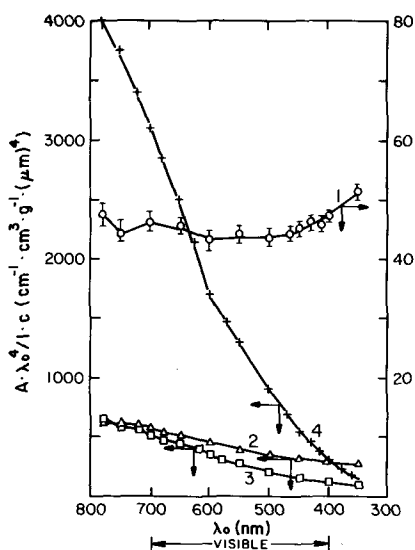
<sup>a</sup>From Table III.<sup>b</sup>From tables in Kratochvil (14).<sup>c</sup>Nominal sphere diameter was 0.091  $\mu\text{m}$ .

FIG. 1B. Wavelength dependence test of specific absorbances of Figure 1A.

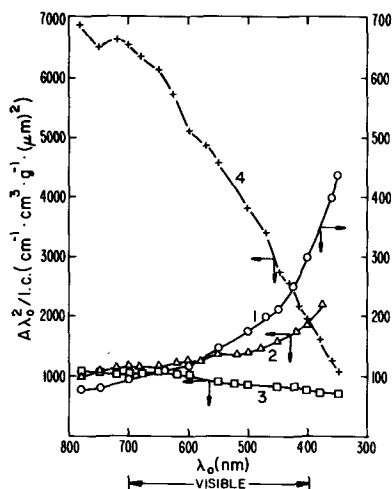


FIG. 1C. Alternate wavelength dependence test of specific absorbances of Figure 1A.

the wavelength dependence of the absorbance measured with commercial spectrophotometers of the sort we employed.

In Figure 1A, we show the absorbance for the four sizes studied. The specific absorbance of the smallest microspheres,  $d = 0.091 \mu\text{m}$ , was the smallest and depended most strongly on wavelength. For these microspheres, the dimensionless size parameter  $\alpha$  ranged from 0.48 to 0.94 (Table II); hence the product  $\alpha m$  ranged from 0.58 to 1.05. Because the conditions (2) for Rayleigh scattering did not hold strictly, (or not at all for  $\alpha m = 1.05$ ), we expected that the measured wavelength exponent  $g$  would be smaller than 4. Kratochvil (14) gives values of the particle dissipation factor  $Q$ , Equation 15, as  $1/1.099$  for  $d/\lambda = 0.15$  and  $1/1.409$  for  $d/\lambda = 0.30$ . We could, therefore, explain for the  $0.091 \mu\text{m}$  microspheres a decrease of ca. 25% of the product  $A\lambda_0^4$  with decreasing wavelength, but in fact we did not observe it; the product  $A\lambda_0^4$  versus  $\lambda_0$  was constant, i.e.,  $g = 4$  (Fig. 1B). Probably the increase of the refractive index ratio with decreasing wavelength compensated the decrease in  $A$  (16).

We measured light scattering from dispersions of  $0.091 \mu\text{m}$  microspheres at increasing concentration and path length in order to examine the effect of multiple scattering. The results are shown in Table III. At the green and blue wavelengths, the dissymmetry was virtually concentration-independent up to absorbances of ca. 0.03, above which it started dropping. At the concentration of 3.25 ppm, the variation of the dissymmetry and the scattering ratio with path length indicates that the observed decrease in dissymmetry and increase in scattering ratio were related to the absorbance, i.e., to the extent of multiple scattering, and not to concentration dependence of scattering. We drew the same conclusion by comparing results at the same concentration and path length but at a second wavelength at which the absorbance was different (the 51.0 ppm entry).

Evidently, multiple scattering leads to a more uniform angular dependence of scattering intensity than does single scattering, in agreement with published calculations (17). The scattering ratio at  $90^\circ$ , Equation 10, which is another sensitive indicator of multiple scattering, increased from its lowest value of 0.02 (which could be an instrumental artifact) to values as high as 0.24 at an absorbance of 0.445 (or a turbidity of 1.02). Multiple scattering is predominant at so high turbidity (11).

If we would interpret the dissymmetry results in terms of single scattering theory (14), we would get diameter values which would appear to decrease with increasing concentration (Table IV), even though the true value remains  $0.091 \mu\text{m}$ . Moreover, a scattering ratio of 0.11 at 546 nm would imply erroneously a larger diameter of  $0.3 \mu\text{m}$  (18). The conclusion is that when there is multiple scattering, i.e., when  $A > 0.04$ , the size cannot be reliably estimated from the angular dependence and the state of polarization of scattered light. On the other hand, the wavelength dependence of absorbance gives a reliable size "fingerprint," for sizes up to  $1.1 \mu\text{m}$  at least, provided the absorbance does not exceed 2. Moreover, simply decreasing the angle of acceptance by placing the detector as far from the sample as is practicable can increase greatly these limits of applicability of spectroturbidimetry. By increasing the distance between sample and detector by a factor of 10, the absorbance limit will increase from 2 to 4, because  $f$  will decrease

## APPEARANCES OF MODEL DISPERSIONS

TABLE V  
Observations of Aqueous Dispersions of Polymer Latex Microspheres of Diameter 0.091  $\mu\text{m}$ : Relation to Spectroturbidimetry (Fig. 1).

Particles concentration (ppm)	Sample Path length (cm)	Photograph in Fig. no.	Observations				Spectroturbidimetry		
			Appearance <sup>a</sup>	Colors		Angular dependence of color <sup>d</sup>	Exponent $g^e$	Scattering regime	
				Scattered light <sup>b</sup>	Scattered or transmitted <sup>c</sup>			650 nm	450 nm
0	2	2A	Clear	Colorless	Colorless	No	—	—	s
21	0.5	—	Clear	Colorless	Colorless	No	4	Rayleigh	s
21	2	2A	Clear	Faint bluish	Faint bluish	No	4	Rayleigh	s
117	1	2B	Translucent-clear	Light bluish	Light bluish or light yellowish	Mild	4	Rayleigh	m-s
117	2	2A	Translucent-clear	Bluish	Bluish or yellowish	Mild	4	Rayleigh	s-m
1,292	1	2B	Turbid-translucent	Bluish-white	Bluish-white or orange	Strong	4	Rayleigh	m
1,292	2	2A	Translucent-turbid	Bluish-white	Bluish-white or orange	Strong	4	Rayleigh	m
1,292	4	—	Turbid	Bluish-white	Bluish-white or orange	Strong	4	Rayleigh	m
100,000	0.5	—	Opaque	Milky white	Milky white	No	Indeterminate <sup>f</sup>	—	m

<sup>a</sup>Appearance can be (5): clear, transparent; translucent, i.e., cloudy or hazy, but one can resolve details by looking at an object through the sample; opaque. By turbid-translucent is meant closer to translucent than to turbid.

<sup>b</sup>Sample observed so that detected light was mainly scattered and not transmitted.

<sup>c</sup>Sample was placed in different positions relative to the light source so that either scattered or transmitted light be observed from different regions of the sample.

<sup>d</sup>Dependence of colors on relative position of source, sample, and observer: related to c.

<sup>e</sup>Exponent  $g$  defined from  $A \propto \lambda_0^{-g}$ .

<sup>f</sup>Depending on turbidity ( $\tau = 2.303A$ ) in the red, 650 nm, or blue, 450 nm, scattering events are: single, s, if  $\tau < 0.1$ ; single and multiple, s-m, if  $0.1 < \tau < 0.3$ ; multiple and single, m-s, if  $0.3 < \tau < 1$ ; and multiple, m, if  $\tau > 1$ .

<sup>g</sup>Absorbance was so high that wavelength dependence could not be interpreted.

TABLE VI  
Observations of Aqueous Dispersions of Polymer Latex Microspheres of Diameter 0.254  $\mu\text{m}$ : Relation to Spectroturbidimetry (Fig. 1).

Particles concentration (ppm)	Sample Path length (cm)	Photograph in Fig. no.	Observations				Spectroturbidimetry			
			Appearance <sup>a</sup>	Colors		Angular dependence of color <sup>d</sup>	Exponent $g^e$	Scattering regime		
				Scattered light <sup>b</sup>	Scattered or transmitted <sup>c</sup>			650 nm	450 nm	
18.3	0.2	—	Clear	Colorless	Colorless	No	$2 < g < 4$	Rayleigh-Debye-Gans	s	s
18.3	0.5	—	Clear	Faint bluish	Faint bluish	No	$2 < g < 4$	Rayleigh-Debye-Gans	s	s-m
18.3	2	2C	Clear	Light bluish	Bluish or Yellowish	Minor	$2 < g < 4$	Debye-Gans	s-m	m-s
18.3	7	—	Translucent	Bluish	Bluish or Yellowish	Medium	$2 < g < 4$	Rayleigh-Debye-Gans	m-s	m
48.3	2	2C	Translucent	Bluish	Bluish or Yellowish	Medium	$2 < g < 4$	Rayleigh-Debye-Gans	m	m
48.3	7	—	Turbid-Translucent	Gray-bluish	Yellowish	Minor	$2 < g < 4$	Rayleigh-Debye-Gans	m	m
463	2	2C	Turbid-opaque	Gray-white	Gray-bluish	Minor	$2 < g < 4$	Rayleigh-Debye-Gans	m	m
463	6	—	Turbid-opaque	Gray-white	Gray-white	Minor	indeterminate <sup>g</sup>	indeterminate <sup>g</sup>	m	m
100,000	0.5	—	Opaque	Milky-white	Milky-white	No	indeterminate <sup>g</sup>	indeterminate <sup>g</sup>	m	m

Footnotes the same as those of Table V.

TABLE VII  
Observations of Aqueous Dispersions of Polymer Latex Microspheres of Diameter 0.325  $\mu\text{m}$ : Relation to Spectroturbidimetry (Fig. 1).

Particles concentration (ppm)	Sample Path length (cm)	Photograph in Fig. no.	Observations				Spectroturbidimetry			
			Appearance <sup>a</sup>	Colors		Angular dependence of color <sup>d</sup>	Exponent $g^e$	Scattering regime		
				Scattered light <sup>b</sup>	Scattered or transmitted <sup>c</sup>			650 nm	450 nm	
8.4	2	2D	Clear	Faint bluish	Faint bluish	No	$1 < g < 2$	Rayleigh-Debye-Gans	s	s-m
68	1	—	Translucent-clear	Light bluish	Light bluish	Mild	$1 < g < 2$	Rayleigh-Debye-Gans	m-s	m-s
68	2	2D	Translucent	Light bluish	Light bluish or Light yellowish	Mild	$1 < g < 2$	Debye-Gans	m-s	m
68	5	—	Translucent-turbid	Faint bluish	Faint bluish or yellowish	Mild	$1 < g < 2$	Rayleigh-Debye-Gans	m	m
900	1	—	Turbid	Gray	Gray or yellowish	Mild	$1 < g < 2$	Rayleigh-Debye-Gans	m	m
900	2	2D	Turbid	Gray	Gray or yellowish	Mild	$1 < g < 2$	Rayleigh-Debye-Gans	m	m
900	5	—	Turbid-opaque	White	Gray or yellowish	Mild	$1 < g < 2$	Rayleigh-Debye-Gans	m	m
100,000	0.5	—	Opaque	Milky-white	Milky-white	No	Indeterminate <sup>g</sup>	Indeterminate <sup>g</sup>	m	m

Footnotes the same as those of Table V.



TABLE VIII  
Observations of Aqueous Dispersions of Polymer Latex Microspheres of Diameter 1.10  $\mu\text{m}$ : Relation to Spectroturbidimetry (Fig. 1).

Particles concentration (ppm)	Sample Path length (cm)	Photograph in Fig. no.	Observations				Spectroturbidimetry			
			Appearance <sup>a</sup>	Colors		Angular dependence of color <sup>d</sup>	Exponent $g^c$	Scattering regime	Scattering events <sup>f</sup>	
				Scattered light <sup>b</sup>	Scattered or transmitted <sup>e</sup>				650 nm	450 nm
4.64	2	3A	Clear	Light gray	Light gray	No	-1 < $g$ < 1	Mie	s-m	s-m
4.64	5	—	Translucent-clear	Light gray	Light gray	No	-1 < $g$ < 1	Mie	m-s	m-s
18.3	2	3A	Translucent	Gray-white	Gray-white	No	-1 < $g$ < 1	Mie	m	m
18.3	5	—	Translucent-turbid	Gray-white	Gray-white	No	-1 < $g$ < 1	Mie	m	m
65.3	2	3A	Turbid	Gray-white	Gray-white	No	-1 < $g$ < 1	Mie	m	m
65.3	5	—	Opaque	Gray-white	Gray-white	No	-1 < $g$ < 1	Mie	m	m
716	2	—	Opaque	Gray-white	Gray-white	No	Indeterminate <sup>g</sup>	Indeterminate <sup>g</sup>	m	m
716	5	—	Opaque	Gray-white	Gray-white	No	Indeterminate <sup>g</sup>	Indeterminate <sup>g</sup>	m	m
100,000	0.5	—	Opaque	Milky-white	Milky-white	No	Indeterminate <sup>g</sup>	Indeterminate <sup>g</sup>	m	m

Footnotes the same as those of Table V.

by a factor of 100 (see Equation 16).

The absorbance of dispersions of the 0.254  $\mu\text{m}$  microspheres increased with decreasing wavelength (Fig. 1A). Since  $A\lambda_0^4$  decreased with decreasing wavelength, whereas  $A\lambda_0^2$  increased, the exponent  $g$  was between 2 and 4 (Figs. 1B and 1C); moreover, because  $g$  varied with wavelength, no attempt was made to fit values of  $g$ . The wavelength dependence was typical of the Rayleigh-Debye-Gans regime, because the basic conditions (11) for this regime were approximately fulfilled:  $m-1 = 0.2$  and  $\alpha(m-1) = 0.27$  to 0.53. For these values, which are not much less than one, the deviations from the R-D-G regime are small.

The wavelength exponent of absorbances of 0.325  $\mu\text{m}$  PMMA dispersions was slightly smaller than 2 (Fig. 1C). These microspheres also scattered light in the Rayleigh-Debye-Gans regime. The specific absorbances were smaller than those of the 0.254  $\mu\text{m}$  microspheres, because the refractive index ratio of PMMA is smaller than that of PS (Table II and Ref. 15).

The 1.10  $\mu\text{m}$  particles scattered in the Mie regime at the wavelengths used, because the Rayleigh and the Rayleigh-Debye-Gans conditions were clearly violated; depending on wavelength,  $\alpha$  ranged from 5.91 to 11.53, and  $\alpha(m-1)$  ranged from 1.18 to 2.31. The wavelength exponent was roughly between 1 and -1. The absorbance maximum (Fig. 1A) occurred at  $\lambda_0 = 500$  nm. For  $m = 1.2$ , the calculated absorbance maximum should occur at  $\alpha = 7.2$  (15). This implies a value of 0.86  $\mu\text{m}$  for the microspheres diameter, which was 20% smaller than the nominal diameter determined from electron microscopy by the manufacturer. Inasmuch as there are often discrepancies of 5-15% between estimates of diameter from electron microscopy and light scattering (4), we judged that agreement between theory and experiment was good.

The measured specific absorbances (Fig. 1) were consistently lower than the calculated absorbances (15). We did not investigate further this discrepancy, because the absolute concentrations were not known precisely and because the wavelength dependence of the absorbance was primarily used to interpret visual observations of scattering colors (5).

Our observations of dispersions are recorded in Tables V-VIII. Figures 2 and 3 are photographs of the same samples. A surprising result was that, under normal laboratory illumination, single scattering could scarcely be detected by the unaided eye. The eye's sensitivity was better in the dark with intense illumination directed toward the sample. For high absorbances, higher than 10, say, most samples looked milky-white, and thus we could obtain no information from their visual appearance alone.

In Rayleigh scattering with absorbances in blue light ranging from 0.05 to 0.2, bluish scattered light was visible and transmitted light was white to yellowish. In order to detect the Tyndall effect, i.e., the bluish colors of scattered light and orange colors of transmitted light in ordinary laboratory illumination, we had to use samples with absorbances in blue light from 0.2 to 2, for which multiple scattering is predominant.

In Rayleigh-Debye-Gans scattering, we saw bluish scattered light and yellowish transmitted light at absorbances of ca. 0.1-1 (Tables VI and VII). The bluish color was less brilliant than the color arising from Rayleigh scattering, because wavelengths other than blue were scattered comparably and decreased the color purity of scattered light. We

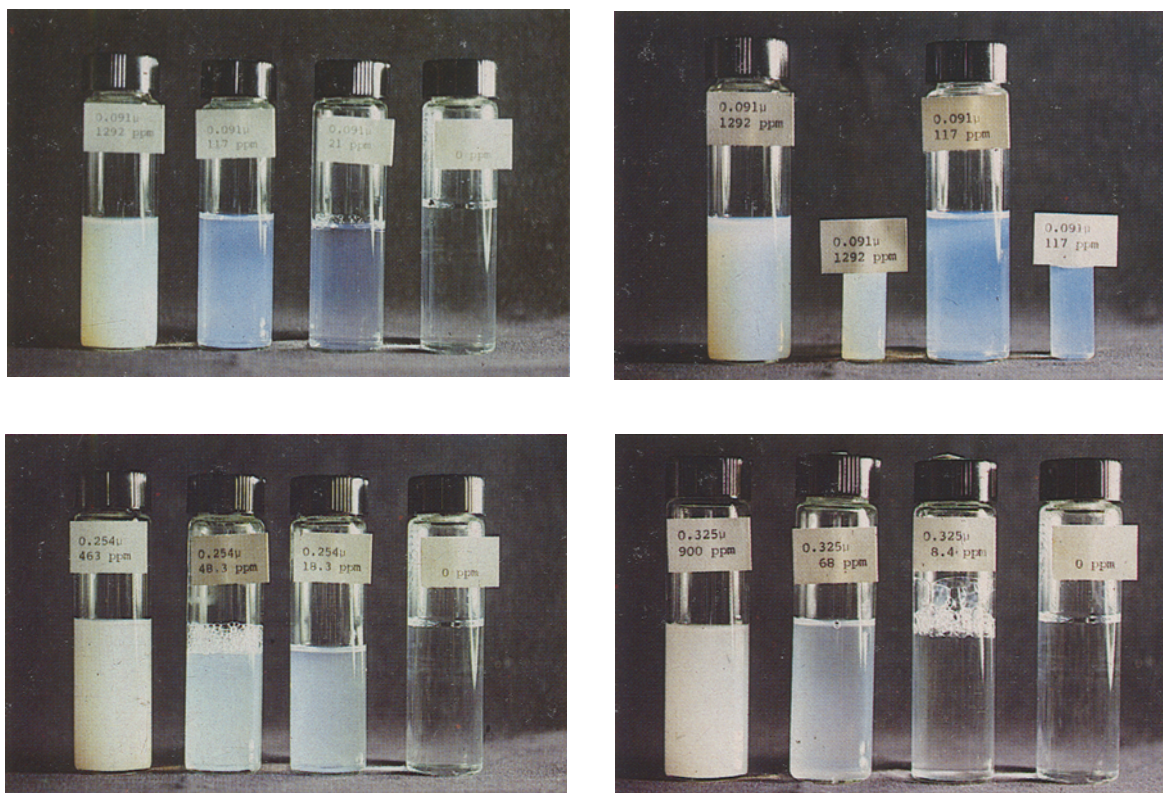


FIG. 2. Photographs of dispersions of polymer latex microspheres. Upper left: 0.091  $\mu\text{m}$  particles of concentrations 1300, 120, 21, and 0 ppm (from left to right); Upper right: 0.091  $\mu\text{m}$ , 1300, 1300, 120, and 120 ppm; Lower left: 0.254  $\mu\text{m}$ , 460, 48, 18, and 0 ppm; Lower right: 0.325  $\mu\text{m}$ , 900, 70, 8 and 0 ppm.

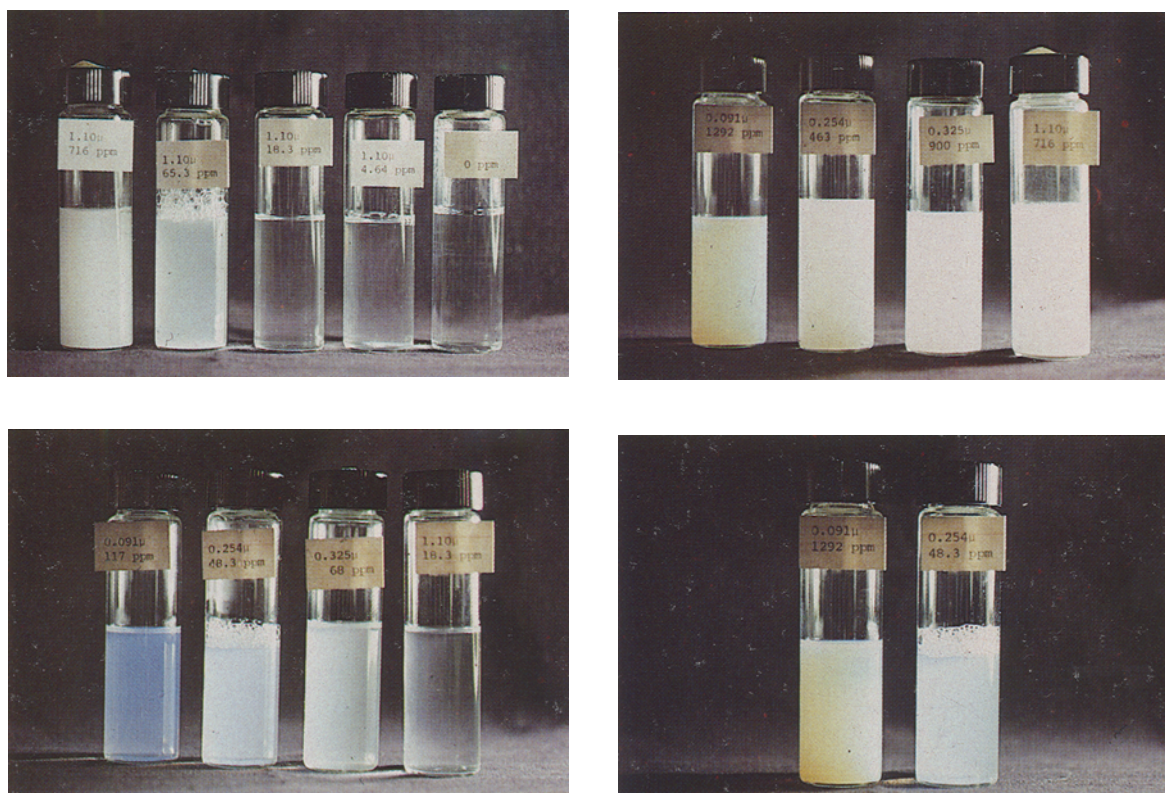


FIG. 3. Photographs of dispersions of polymer latex microspheres. Upper left: 1.10  $\mu\text{m}$ , 720, 65, 18, 4.6, and 0 ppm; Upper right: 0.091  $\mu\text{m}$  - 1300 ppm, 0.254  $\mu\text{m}$  - 460 ppm, 0.325  $\mu\text{m}$  - 900 ppm, 1.10  $\mu\text{m}$  - 720 ppm; Lower left: 0.091  $\mu\text{m}$  - 120 ppm, 0.254  $\mu\text{m}$  - 28 ppm, 0.325  $\mu\text{m}$  - 70 ppm, 110  $\mu\text{m}$  - 18 ppm, 0.091  $\mu\text{m}$  - 1300 ppm, 0.254  $\mu\text{m}$  - 48 ppm.

## APPEARANCES OF MODEL DISPERSIONS

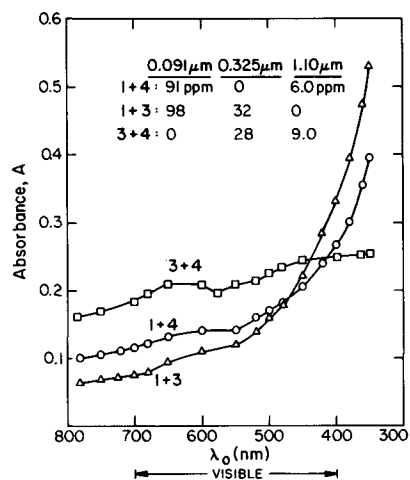


FIG. 4A. Spectra of absorbance, through 1 cm path length, of dispersions of mixtures of microspheres with different size.

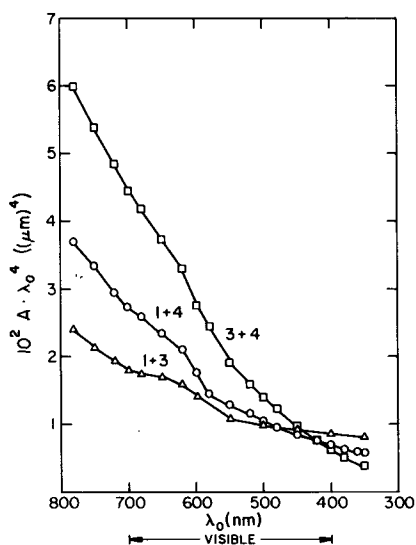


FIG. 4B. Wavelength dependence test of absorbances of Figure 4A.

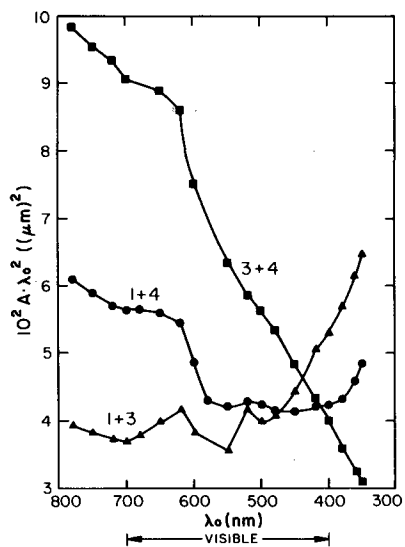


FIG. 4C. Alternate wavelength dependence test of absorbances of Figure 4A.

TABLE IX

Observations of Aqueous Dispersions of Mixtures of Monodisperse Polymer Latex Microspheres: Relation to Spectroturbidimetry (Fig. 4).

Sample			Observations			Spectroturbidimetry			
Concentration (ppm)			Colors			Exponent g <sup>c</sup>	Scattering regime	Scattering events <sup>f</sup>	
0.091 μm	0.325 μm	0.10 μm	Appearance <sup>a</sup>	Scattered light <sup>b</sup>	Scattered or transmitted <sup>c</sup>			Angular dependence of color <sup>d</sup>	650 nm
91	0	6.0	Translucent-clear	Bluish	Bluish or light yellowish	Mild	~2(<2)	Rayleigh-Debye-Gans	m-s
91	0	6.0	Clear-translucent	Bluish	Bluish or yellowish	Medium	~2(<2)	Rayleigh-Debye-Gans	m-s
98	32	0	Clear-translucent	Bluish	Bluish or light yellowish	Mild	~2(>2)	Rayleigh-Debye-Gans	m-s
98	32	0	Translucent	Bluish or yellowish	Bluish or yellowish	Medium	~2(>2)	Rayleigh-Debye-Gans	m
0	28	9.0	Translucent	Grayish-faint bluish	Grayish-faint bluish	Minor	~1	Mie	m-s
0	28	9.0	Translucent	Grayish-faint bluish	Grayish-faint bluish	Minor	~1	Mie	m

Footnotes the same as those of Table V.

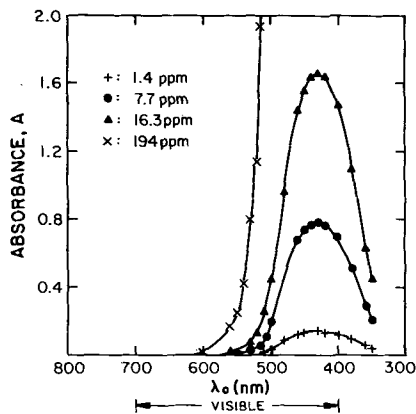


FIG. 5. Spectra of absorbance, through 1 cm path length, of aqueous methyl red dye.

TABLE X

Colors of Clear Aqueous Solutions of Methyl Red Dye: Relation to Absorption Spectrum (Fig. 5)

Concentration (ppm)	Path length (cm)	Perceived color	% Pure color absorbed					
			Red	Orange	Yellow	Green	Blue	Violet
0.36	<1	None	<1	<1	<1	<1	1-6	6-8
1.4	0.2	None	<1	<1	<1	<1	1-5	5-7
1.4	0.5	Faint yellow	<1	<1	<1	1-4	4-14	14-20
1.4	2 <sup>a</sup>	Faint yellow	<1	<1	<1	1-15	15-45	45-50
1.4	5	Light yellow	<1	<1	<1	1-35	35-80	80-85
7.7	2 <sup>a</sup>	Yellow	<1	<1	<1	1-60	60-97	96-97
7.7	5	Yellow	<1	<1	<1	4-90	90-99+	99+
16.3	2 <sup>a</sup>	Yellow	<1	<1	1-7	7-87	87-99+	99+
16.3	5	Yellow to light orange	<1	<1	3-11	11-99+	99+	99+
194	1	Light orange	<1	1-9	9-24	24-99+	99+	99+
194	2 <sup>a</sup>	Orange	0-2	2-20	20-84	84-99+	99+	99+
194	5	Dark orange	0-5	5-37	37-84	84-99+	99+	99+
2650	0.5	Red to orange	0-8	8-50	50-90	90-99+	99+	99+
2650	2	Red	0-38	38-90	90-99+	99+	99+	99+
2650	6	Dark red	0-75	75-99+	99+	99+	99+	99+

<sup>a</sup>Photographs of these samples are shown in Figure 7.

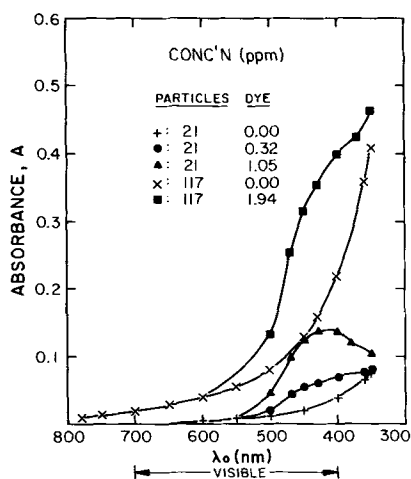


FIG. 6A. Spectra of absorbance, through 1 cm path length, of 0.091  $\mu\text{m}$  polymer latex microspheres in aqueous methyl red dye.

could see no color in dispersions of Mie microspheres (Table VIII), which is as predicted from the weak wavelength dependence of absorbance.

By comparing appearances of dispersions of microspheres of widely different sizes (Fig. 3B), we determined that little information could be obtained at absorbances higher than 3. However, by comparing dispersions with about the same absorbance in the range 0.1-1, we could tell that they differed in size. Figure 3D shows that if  $A > 1$ , a high concentration of smaller microspheres could give rise to a less brilliant blue than the scattering bluish color arising from larger particles, and thus could lead to the erroneous conclusion that the particle size was larger.

Thus, careful naked-eye observations of dispersions of monodisperse particles can give qualitative information in agreement with that given by spectroturbidimetry. The latter is surely more reliable and more sensitive.

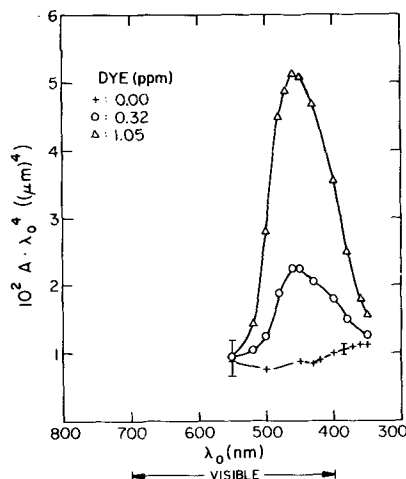


FIG. 6B. Wavelength dependence test of absorbances of dispersions of 0.091  $\mu\text{m}$  microspheres, 21 ppm, in aqueous methyl red dye, Figure 6A.

TABLE XI  
Observations of Aqueous Dispersions of Polymer Latex Microspheres with Added Methyl Red Dye (Figs. 6 and 7)

Diameter ( $\mu\text{m}$ )	Particles Concentration (ppm)	Dye Concentration (ppm)	Appearance		Dye only	Colors		Angular dependence color			
			Particles with dye (1)	Particles only (2)		Scattered light (1)	(2)	(1)	(2)		
0.091	1179	17	Turbid-translucent	Turbid-translucent	Yellow	Orange & green	Bluish-white	Yellow or orange	Bluish-white or orange	Strong	Strong
0.091	142	173	Translucent	Translucent	Orange	Orange	Bluish	Orange	Bluish or yellowish	No	Medium
0.091	117	0.36	Translucent-clear	Translucent-clear	None	Light bluish & faint yellowish	Bluish	Bluish or yellowish	Bluish or yellowish	Medium	Mild
0.091	117	1.94	Translucent-clear	Translucent-clear	Faint yellow	Yellowish	Bluish	Bluish or yellowish	Bluish or yellowish	Mild	Mild
0.091	21	0.32	Clear	Clear	None	Faint bluish	Faint bluish	Faint bluish or yellowish	Faint bluish	Mild	No
0.091	21	1.05	Clear	Clear	Faint yellow	Faint yellowish	Faint bluish	Yellowish	Faint bluish	Mild	Mild
0.325	900	1.27	Turbid	Turbid	Faint yellow	Yellow	Gray	Yellow or gray	Grayish or yellow	Mild	Mild
1.10	63	7.2	Turbid	Turbid	Yellow	Yellow	Gray-white	Yellow	Gray-white	No	No

### Dispersions of Mixtures of Microspheres with Different Size

Absorbance measurements and visual observations were designed to probe whether one can detect particles of one size in the presence of particles of another size. Spectra of absorbances of three dispersions of pairs of sizes are shown in Figure 4. Concentrations were chosen so that, for path lengths 1 cm and 2 cm, absorbances fall in the range 0.1-1, which we found to be the best range for observing by unaided eye. The measured absorbances were equal to within 10% to the sum of the absorbances calculated from Figure 1 and from the particle concentrations. The wavelength exponent for 91 ppm microspheres of diameter  $0.091 \mu\text{m}$  dropped from 4 to ca. 2 upon addition of just 6 ppm of microspheres of  $1.10 \mu\text{m}$ . Thus one cannot distinguish from  $g$  values alone between a mixture of Rayleigh and Mie particles and Rayleigh-Debye-Gans particles; calculations are necessary. Nevertheless, spectroturbidimetry can readily detect particles of sizes larger than  $0.1 \mu\text{m}$  merely from the wavelength exponent. For the  $1.10 \mu\text{m}$  microspheres, concentrations as low as 6 ppm can be detected.

Visual observations are described in Table IX. Translucency and lack of bluish scattering colors indicated correctly the absence of Rayleigh particles, i.e., indicated particles of sizes larger than  $0.1 \mu\text{m}$  in the sample with the  $0.325$  and  $1.10 \mu\text{m}$  microspheres.

### Dispersions of Microspheres with Dye Added

Absorbance spectra of aqueous methyl red dye with 0.21% SDS added are shown in Figure 5. The specific absorbance  $A/c$  was independent of concentration within experimental precision and it therefore followed Beer's law. The molar absorptivity at the wavelength  $\lambda_{\text{max}} = 430 \text{ nm}$  of maximum intensity was found to be  $\epsilon_{\text{max}} = 3.03 \times 10^4 \text{ L}\cdot\text{mol}^{-1}\cdot\text{cm}^{-1}$ .

Because the absorption peak was wide, the higher the absorbance the more important was the reduction of intensity at wavelengths around the wavelength  $\lambda_{\text{max}}$ . Table X shows the percentage of light absorbed for each color band. The perceived color of the samples resulted, of course, from selective reduction of intensity at some wavelengths in the spectrum of the illuminating source. Colors ranged from faint yellow to dark red. When  $A_{\text{max}} < 0.05$ , no color was discernible.

Figure 6 shows absorbance spectra of  $0.091 \mu\text{m}$  microspheres with various concentrations of dye. The measured absorbance was equal to the sum of  $A_{\text{abs}}$  by the dye and  $A_{\text{scat}}$  by the particles. The product  $A\lambda_0^4$  started increasing substantially below  $550 \text{ nm}$  (Fig. 6B), thus enabling us to detect correctly the wavelength range at which absorption was significant (Fig. 5).

When dye was present as well as Rayleigh particles, absorption colors were mixed with Rayleigh scattering colors (Table XI and Fig. 7). The result of the mixing of colors depended on the hue and relative luminosity of the components (5). Because the scattered color varied with the angle between the direction of illumination and the direction of observation, i.e., on the relative position of light source, sample, and observer, the mixed color depended on this angle. The Tyndall effect was thus affected by the absorption color and was totally suppressed when absorption was sufficiently strong (second entry in Table XI). Also shown in Figure 7 is a turbid dispersion of 63 ppm  $1.10$





FIG. 7. Photographs of dispersions of polymer latex microspheres, dye solutions, and mixtures of them. Upper left: 0.091  $\mu$ m particles and dye of respective concentration in ppm 1200-17, 0-16, and 1300-0; Upper right: same with concentrations 120-1.9, 120-0.36, 120-0, and 0-1.4; Lower left: same, 21-0.32, 21-1.05, and 12-0; Lower right: 0.325  $\mu$ m - 900 ppm with 1.27 ppm of dye, 0.325  $\mu$ m - 900 ppm with no dye 1.4 ppm dye with no particles, 1.10  $\mu$ m - 63 ppm and 7.2 ppm dye, 1.10  $\mu$ m - 65 ppm, and dye 7.7 ppm.

$\mu$ m microspheres with 7.2 ppm dye. Its absorbance spectrum (not shown) has a maximum. Because scattering can cause such maxima (15), the observed maximum does not necessarily imply absorption. The plot (not shown) of  $\Delta\lambda_0^4$  versus  $\lambda_0$  decreased monotonically with decreasing wavelength, providing no clue to absorption either. However, the color of the dispersion, yellow and independent of angle, could not be accounted for by scattering alone and thus must have been due to absorption. This was a relatively rare case in which the visual observation was more sensitive than spectroturbidimetry for detecting the absorption.

#### ACKNOWLEDGMENT

The National Science Foundation and the Department of Energy provided financial support for this work.

#### REFERENCES

- Prince, L.M., in *Emulsions and Emulsion Technology*, edited by K.J. Lissant, Marcel Dekker, New York, 1974, p. 125.
- Griffin, W.C., in *Encyclopedia of Chemical Technology*, 2nd edn., Vol. 8, Wiley, New York, 1965, p. 117.
- Kerker, M., *The Scattering of Light and Other Electromagnetic Radiation*, Academic Press, New York, 1969, Chap. 7.
- Van den Hul, H.J., and J.W. Vanderhoff, in *Polymer Colloids*, edited by R.M. Fitch, Plenum Press, New York, 1971, p. 1.
- Frances, E.I., L.E. Scriven, W.G. Miller and H.T. Davis, *JAOCS* 60:1043 (1983).
- Frances, E.I., H.T. Davis, W.G. Miller and L.E. Scriven, in *Chemistry of Oil Recovery*, edited by R. Johansen and R.L. Berg, ACS Symposium Series 91, American Chemical Society, Washington, DC, 1979, p. 35.
- Puig, J.E., E.I. Frances, H.T. Davis, W.G. Miller and L.E. Scriven, *Soc. Pet. Eng. J.* 19:71 (1979).
- Frances, E.I., Y. Talmon, L.E. Scriven, H.T. Davis and W.G. Miller, *J. Colloid Interface Sci.* 82:449 (1982).
- Meehan, E.J., *Optical Methods of Analysis*, Part I, vol. 5, reprinted from *Treatise on Analytical Chemistry*, edited by J.M. Kolthoff and P.J. Elving, Wiley, New York, 1964, p. 2707.
- Cardinal, J.R., and P. Mukerjee, *J. Phys. Chem.* 82:1614 (1978).
- Van de Hulst, H.C., *Light Scattering by Small Particles*, Wiley, New York, 1957, pp. 6-133.
- Tanford, C., *Physical Chemistry of Macromolecules*, Wiley, New York, 1961, pp. 282,287.
- Sudhakar, Y., M.S. thesis, in progress, Purdue University, IN.
- Kratochvil, P., in *Light Scattering from Polymer Solutions*, edited by M.B. Huglin, Academic Press, London, 1972, p. 333.
- Heller, W., and H.J. McCarty, *J. Chem. Phys.* 29:78 (1958).
- Heller, W., H.L. Bhatnagar and M. Nakagaki, *J. Chem. Phys.* 36:1163 (1962).
- Kortum, G., *Reflectance Spectroscopy*, Springer Verlag, Berlin, 1969, p. 94.
- Heller, W., and R. Tabibian, *J. Phys. Chem.* 63:2059 (1962).
- Goulden, J.D.S., *Brit. J. Appl. Phys.* 12:456 (1961).
- Walstra, P., *Ibid.* 16:1187 (1965).
- Huglin, M.B., in *Light Scattering from Polymer Solutions*, edited by M.B. Huglin, Academic Press, London, 1972, p. 255.

[Received October 10, 1982]